On the stereoselectivity of 4-penten-1-oxyl radical 5-*exo*-trig cyclizations†‡

Jens Hartung,*[a] Kristina Daniel,[a] Christian Rummey[b] and Gerhard Bringmann[b]

Received 8th August 2006, Accepted 22nd September 2006
First published as an Advance Article on the web 16th October 2006
DOI: 10.1039/b611473c

Ring closure reactions were investigated in a combined computational (density functional theory) and experimental study, to uncover the origin of diastereoselection in 5-*exo*-trig cyclizations of methyl and *tert*-butyl-substituted 4-penten-1-oxyl radicals. Selectivity data were calculated on the basis of transition state theory, the Curtin–Hammett principle, and Maxwell–Boltzmann statistics, to provide an excellent correlation between computed and experimental *cis*–*trans* ratios. The data show that the 2,3-*trans*-, 2,4-*cis*-, and 2,5-*trans*-diastereoselection exerted by CH_3 and $C(CH_3)_3$ groups increases along substituent positions 1 < 2 < 3, with the effect of *tert*-butyl substituents being more pronounced. Theory states that the favored mode of cyclization proceeds *via* intermediates that are characterized by an offset of atoms C2 and C3 into opposite directions from the plane of O1 (radical center)/C5 (olefinic C)/C4 (allylic C). This arrangement allows alkyl substituents and the $=CH_2$ entity to adopt positions that are associated with the fewest and least severe *synclinal* and *synperiplanar* interactions. A transition structure notation is proposed based on conformational characteristics of the heterocycle, the intermediates structurally resemble the closest, *i.e.* tetrahydrofuran.
The new transition state model serves as an alternative to cyclohexane-based guidelines and adequately addresses hitherto unsettled instances properly, such as the lack in diastereoselectivity observed in the 1-phenyl-4-penten-1-oxyl radical 5-*exo*-trig ring closure.

Introduction

Substituted 4-penten-1-oxyl radicals undergo efficient 5-*exo*-trig cyclizations.[1–3] The reaction poses a useful complement to electrophile-induced alkenol ring closures because it is able to provide regio- and diastereoselectivities not attainable in ionic transformations.[4–7] A general guideline states that intermediates with an alkyl substituent attached at position 1 or 3 (*e.g.* **1a**, **1e**) cyclize *trans*-5-*exo*-trig selectively, whereas 2-substituted derivatives (*e.g.* **1c**) prefer the *cis*-5-*exo*-trig mode of ring closure (Scheme 1).[3a] Multiple substitution may increase or decrease stereoselection, depending on the relative configuration of stereocenters.[4] The selectivity in alkenoxyl radical cyclizations has so far been interpreted in extension to the Beckwith–Schiesser–Houk–Spellmeyer model,[8–10] which was introduced several years ago for predicting preferred stereochemical pathways in carbon radical 5-*exo*-trig ring closures. The model takes differences in steric effects into account that originate from axially and equatorially oriented substituents attached to folded conformers of open chain radicals, which resemble either the chair or the boat arrangement of cyclohexane. A quantitative analysis in this type of cyclization is feasible

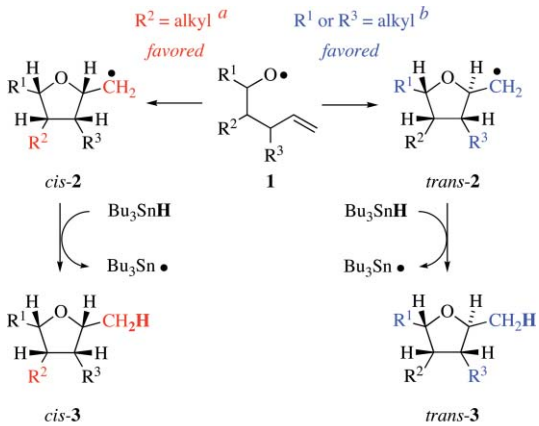

1–3	R^1	R^2	R^3
a	CH_3	H	H
b	$C(CH_3)_3$	H	H
c	H	CH_3	H
d	H	$C(CH_3)_3$	H
e	H	H	CH_3
f	H	H	$C(CH_3)_3$

Scheme 1 Modes of 5-*exo*-trig cyclization of 1-, 2-, and 3-substituted 4-penten-1-oxyl radicals **1** and indexing of *O*-radicals **1**, tetrahydrofuryl-2-methyl radicals *cis*/*trans*-**2**, and tetrahydrofurans *cis*/*trans*-**3**. [a] R^1 and R^3 = H; [b] either R^1 and R^2 or R^2 and R^3 = H.

[a]*Fachbereich Chemie, Organische Chemie, Technische Universität Kaiserslautern, Erwin-Schrödinger-Straße, D-67663, Kaiserslautern, Germany. E-mail: hartung@chemie.uni-kl.de; Fax: +49 631 205 3921*
[b]*Institut für Organische Chemie, Universität Würzburg, Am Hubland, D-97074, Würzburg, Germany*

† Electronic supplementary information (ESI) available: Experimental procedure for the synthesis of alkenyl tosylate **5f**, synthesis and spectral data of tetrahydrofurans *cis*-**3d**, *trans*-**3d**, and *trans*-**3f**, atomic coordinates of radicals **1–2** and intermediates **7–10**, UHF/6-31+G* computed energies and geometrical parameters of radicals **1–2** and intermediates **7–10**, *A*-value analysis of methyl and *tert*-butyl-substituted tetrahydropyrans (B3LYP/6-31+G*), and atomic coordinates of the chair conformation of cyclohexane and distinguished conformers of cyclopentane (B3LYP/6-31G*) (PDF). See DOI: 10.1039/b611473c

‡ Dedicated to Prof. Dr Dr h. c. Waldemar Adam on the occasion of his 69th birthday in recognition of his contributions to the chemistry of reactive oxygen intermediates.

using approximations implemented into two different force field approaches.[8,9] In view of the significance of this model, the origin of diastereoselectivity in 5-*exo*-trig carbon radical cyclizations was addressed in the following years using the MNDO wavefunction, however, without providing additional decisive results.[11] In a series of upcoming contributions, alternative semiempirical wavefunctions were assessed. The selected methods (AM1, PM3), however, were found not to be adequate to correlate computed and experimental selectivity data.[12] In view of this background, the pursuit of selectivity in radical chemistry was continued on different levels of *ab initio* theory [UHF and density functional (DF)]. Thus, stereochemical aspects associated with the Ueno–Stork reaction were explained, and the debate on the stereoselectivity of the 1-*tert*-butyl-5-hexen-1-yl radical ring closure was settled using such methods.[13] Application of *ab initio* theory also contributed to answer longstanding questions on the origin of regioselectivity in cyclizations of the nucleophilic 5-hexen-1-yl radical, the *N*-methyl-4-penten-1-aminyl radical and in particular electrophilic 4-substituted 4-penten-1-oxyl radicals.[12,14–16] In one of these studies it was documented that DF theory (B3LYP/6-31+G*) is able to reproduce experimentally observed regioselectivities in 4-penten-1-oxyl radical cyclizations with a remarkable precision. It further became evident that computed 5-*exo*-trig transition structures resemble distorted tetrahydrofuran conformers more closely than chair or boat conformers of tetrahydropyran.[14] In view of this background and the growing significance of alkenoxyl radical cyclizations in stereoselective synthesis,[5] the origin of diastereoselectivity in cyclizations of 1-, 2-, and 3-alkyl-substituted 4-penten-1-oxl radicals was explored in the present contribution. Since methyl and *tert*-butyl groups serve in conformational analysis as an archetype for sterically small (CH_3) and demanding groups [$C(CH_3)_3$], likewise substituted alkenoxyl radicals were selected with the aim (i) to qualitatively and quantitatively reproduce experimentally measured diastereoselectivities in 4-penten-1-oxyl radical 5-*exo*-trig ring closures, and (ii) to uncover common structural motifs of relevant transition structures on the basis of a tetrahydrofuran-derived conformational analysis, in order to predict selectivities in upcoming stereoselective syntheses using this type of ring closure reaction.

Results

1 Preparation and photochemical conversion of alkoxyl radical precursors§

On the basis of previous studies, *N*-(alkoxy)-4-(*p*-chlorophenyl)-thiazolethiones **6** were selected as alkoxyl radical precursors.[3] The compounds necessary to supplement the existing set of selectivities were prepared as follows. *N*-[2-(*tert*-butyl)-4-penten-1-oxy]-4-(*p*-chlorophenyl)thiazole-2(3*H*)thione (**6d**) was obtained in 80% yield by treatment of *N*-(hydroxy)-4-(*p*-chlorophenyl)thiazole-2(3*H*)-thione tetrabutylammonium salt (**4**)[17,18] with 2-(*tert*-butyl)-4-penten-1-yl *p*-toluenesulfonate (**5d**)[19] in anhydrous DMF (Table 1). In a similar way, *N*-[3-(*tert*-butyl)-4-penten-1-oxy]-4-(*p*-chlorophenyl)thiazole-2(3*H*)thione (**6f**) was isolated in 74% yield

§ The following abbreviations have been used: CP = *p*-chlorophenyl, T = twist conformer, ZPVE = zero-point vibrational energy. Chiral *N*-(alkoxy)thiazolethiones **6d** and **6f** were prepared as racemates and used as such thus leading to racemic products.

Table 1 Preparation of *N*-[(*tert*-butyl)pentenoxy]-4-(*p*-chlorophenyl)-thiazole-2(3*H*)-thiones **6** (CP = *p*-ClC_6H_4)

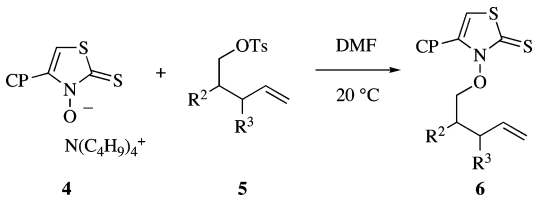

4 **5** **6**

Entry	**5**, **6**	R^2	R^3	Yield of **6** [%]
1	**d**	$C(CH_3)_3$	H	80
2	**f**	H	$C(CH_3)_3$	74

from the reaction between ammonium salt **4** and 3-(*tert*-butyl)-4-penten-1-yl *p*-toluenesulfonate (**5f**) (Table 1 and ESI†). All thiazolethiones **6** were obtained as colorless and crystalline air-stable materials, which were stored in standard glassware in a refrigerator.

Photolysis (350 nm) of a solution of *N*-[2-(*tert*-butyl)-4-penten-1-oxy]-4-(*p*-chlorophenyl)thiazolethione **6d** and Bu_3SnH (c_o = 0.18 M, 2.2 equiv.) in $C_6H_5CF_3$ (20 °C, Scheme 2) provided 96% of 4-(*tert*-butyl)-2-methyltetrahydrofuran (**3d**) as a mixture of *cis–trans*-isomers (GC, *cis–trans* = 90 : 10; for stereochemical analysis see the Discussion) and ≤2% of 2-*tert*-butyl-4-penten-1-ol (GC).[20] A control experiment that was performed by photolyzing (350 nm) a solution of *N*-(2-*tert*-butyl-4-pentenoxy)thiazolethione **6d** and Bu_3SnH in C_6D_6 (20 °C) furnished similar yields of tetrahydrofuran **3d** (*cis–trans* = 90 : 10) and 2-*tert*-butyl-4-penten-1-ol (^{1}H NMR, anisole as internal standard). Work up of this reaction mixture afforded 73% of tetrahydrofuran **3d** as a colorless volatile liquid.

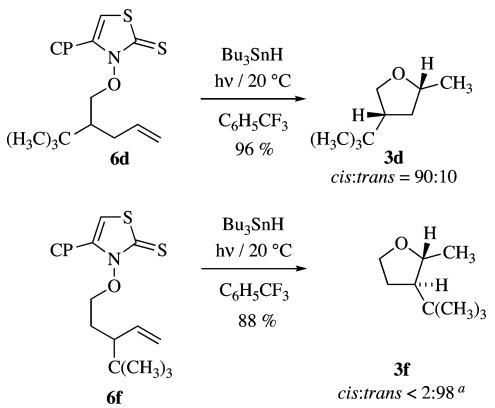

Scheme 2 Synthesis of 4-(*tert*-butyl)-2-methyltetrahydrofuran **3d** and 3-(*tert*-butyl)-2-methyltetrahydrofuran **3f** from *N*-[(*tert*-butyl)pentenoxy)-thiazolethiones **6d** and **6f**. [a] *cis*-**3f** was not detected (^{1}H NMR).

Photolysis (350 nm, 20 °C) of a solution of *N*-[3-(*tert*-butyl)-4-penten-1-oxy]-4-(*p*-chlorophenyl)thiazole-2(3*H*)thione (**6f**) and Bu_3SnH (c_o = 0.18 M, 2.2 equiv.) in either $C_6H_5CF_3$ (GC-analysis) or C_6D_6 (^{1}H NMR-analysis) afforded 88% of 3-(*tert*-butyl)-4-methyltetrahydrofuran (**3f**) and ≤2% of 3-(*tert*-butyl)-4-penten-1-ol.[21] Purification of the latter reaction mixture furnished 73% of tetrahydrofuran *trans*-**3f** (*cis* : *trans* < 2 : 98, ^{1}H NMR) as a colorless volatile liquid.

2 Theoretical considerations and computational studies

According to an assessment of methods that are adequate to reliably reproduce relative heats of formation in carbon- and oxygen-radical additions to olefins performed by others,[14,16,22,23] and the excellent correlation between experimentally observed and computed regioselectivities in 4-penten-1-oxyl radical cyclizations in a previous study,[14] we restricted ourselves to the use of Becke's three parameter hybrid functional (B3LYP)[24,25] and the 6-31+G* valence basis set for the present investigation.[26,27] The latter includes diffuse *and* polarization wave functions, which are necessary to adequately reproduce selectivities in this type of reaction (for UHF-calculated data, refer to the ESI†).[22]

Selectivity data in 4-penten-1-oxyl radical cyclizations were calculated on the basis of transition state theory, the Curtin–Hammett principle, and Maxwell–Boltzmann statistics.[28,29] Transition state theory is applicable, since *O*-radical cyclizations proceed irreversibly under the conditions applied to measure the data referred to in the present work.[30] The Curtin–Hammett principle states that free-energy differences between reactive conformational isomers must be one order of magnitude smaller than the activation free-energy of a succeeding reaction, *i.e.* the intramolecular *O*-radical addition in the present case. According to this guideline, reactive conformers can be assumed to equilibrate with a sufficiently high rate constant, in order to maintain the equilibrium throughout the reaction, in spite of a continuous loss of reactants. The ratio of products formed from this ensemble then is given by Maxwell–Boltzmann statistics on the basis of Gibbs free-energy differences of associated transition states. In order to keep computational time at a reasonable level without losing essential information, the set of transition states was approximated by the two lowest in energy and therefore most significantly populated transition structures for the *cis- and* for the *trans*-5-*exo*-trig mode of ring closure of radicals **1a–f** (Schemes 3, 4, 5). Torsional movements about secondary C(sp^3),C(sp^3)-bonds are considered to proceed by a factor of 10 faster than cyclizations **1** → *cis*/*trans*-**2** ($k \sim 10^8$ s^{-1} for 303 K).[31] Conformational interchanges occurring by rotation

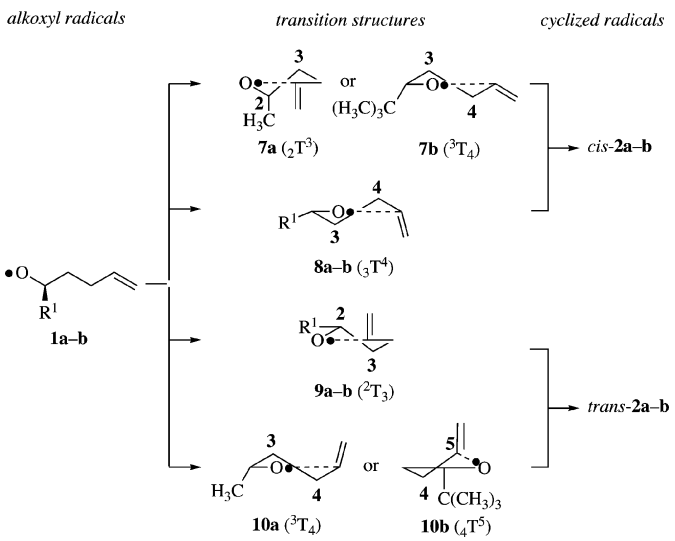

Scheme 3 Relevant transition structures for *cis*- and *trans*-5-*exo*-trig cyclizations of 1-alkyl-substituted 4-penten-1-oxyl radicals **1a–1b** [R^1 = CH_3, $C(CH_3)_3$].

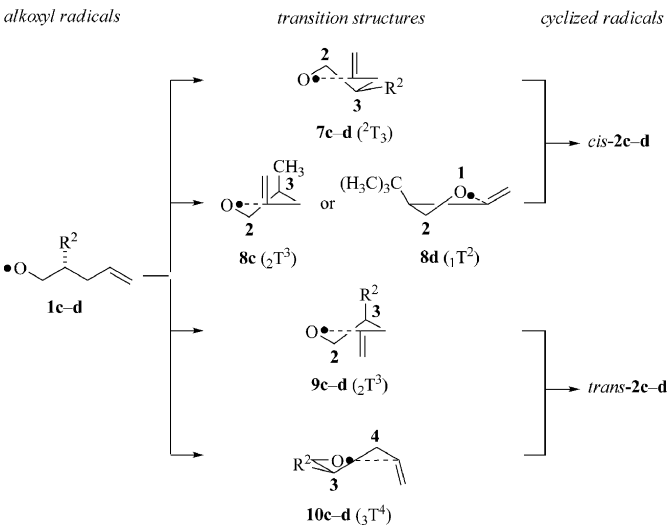

Scheme 4 Relevant transition structures for *cis*- and *trans*-5-*exo*-trig cyclizations of 2-alkyl-substituted 4-penten-1-oxyl radicals **1c–1d** [R^2 = CH_3, $C(CH_3)_3$].

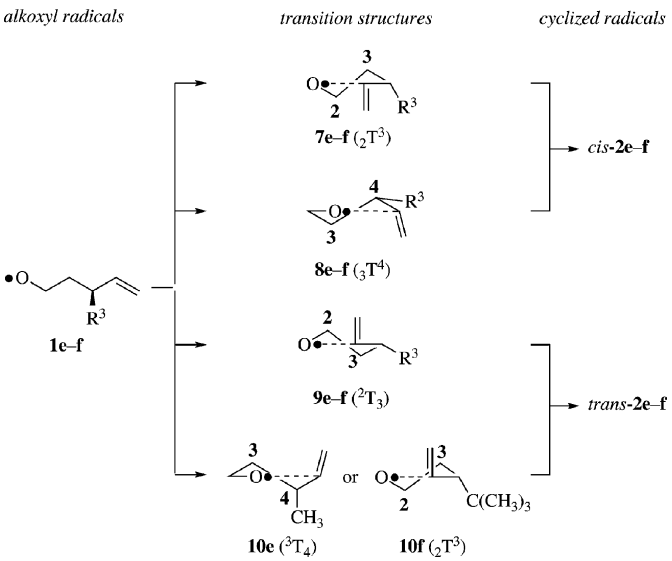

Scheme 5 Relevant transition structures for *cis*- and *trans*-5-*exo*-trig cyclizations of 3-alkyl-substituted 4-penten-1-oxyl radicals **1e–1f** [R^3 = CH_3, $C(CH_3)_3$].

across tertiary C(sp^3),C(sp^3)-bonds, however, may not be too far off from rate constants of intramolecular *O*-radical additions. An assessment of this aspect is outlined in section 4 of the Discussion.

Input coordinates for calculating equilibrium geometries of substituted 4-penten-1-oxyl radicals **1a–f** were obtained in two steps. Global minima from a usage directed conformational search using the MM+ force field[32,33] were taken as starting points for performing subsequent DF calculations.[26] The absence of imaginary harmonic frequencies pointed to minimum structures for alkenoxyl radicals **1** and also for tetrahydrofuryl-2-methyl radicals *cis*/*trans*-**2** on the corresponding potential surfaces. The computed heats of formation (E + ZPVE), zero-point vibrational energies (ZPVE), expectation values of associated spin operators ($\langle S^2 \rangle$), and relative heats of formation ($\Delta\Delta H_f$) of radicals **1** and *cis*/*trans*-**2** are listed in Table 2. An illustration of calculated equilibrium

Table 2 Computed heats of formation (E + ZPVE), zero-point vibrational energies (ZPVE), $\langle S^2 \rangle$-values, and relative heats of formation ($\Delta\Delta H_f$) of radicals **1** and *cis–trans*-**2**[a]

	Parameter	**1**	*cis*-**2**	*trans*-**2**
1a → *cis*-**2a** + *trans*-**2a**	E + ZPVE[b]	−310.251825	−310.270327	−310.270666
	ZPVE[c]	411718.2	415030.0	414574.8
($R^1 = CH_3$)	$\langle S^2 \rangle$	0.7537	0.7539	0.7539
	$\Delta\Delta H_f$ [d]	≡ 0	−48.6	−49.5
	Conformer[e]	—[f]	$^1T_5$	$_3T^4$
1b → *cis*-**2b** + *trans*-**2b** [$R^1 = C(CH_3)_3$]	E + ZPVE[b]	−428.108797	−428.127556	−428.127776
	ZPVE[c]	633449.9	637067.3	636879.9
	$\langle S^2 \rangle$	0. 7538	0.7539	0.7539
	$\Delta\Delta H_f$ [d]	≡ 0	−49.3	−49.8
	Conformer[e]	—[f]	$^1T_5$	$_3T^4$
1c → *cis*-**2c** + *trans*-**2c** ($R^2 = CH_3$)	E + ZPVE[b]	−310.249835	−310.266203	−310.265110
	ZPVE[c]	407212.0	414798.3	414673.9
	$\langle S^2 \rangle$	0.7537	0.7539	0.7538
	$\Delta\Delta H_f$ [d]	≡ 0	−43.0	−40.1
	Conformer[e]	—[f]	$_3T^4$	$_3T^4$
1d → *cis*-**2d** + *trans*-**2d** [$R^2 = C(CH_3)_3$]	E + ZPVE[b]	−428.099582	−428.120857	−428.120004
	ZPVE[c]	634727.3	637842.9	638426.3
	$\langle S^2 \rangle$	0.7561	0.7539	0.7539
	$\Delta\Delta H_f$ [d]	≡ 0	−55.9	−53.6
	Conformer[e]	—[f]	$^2T_3$	$_1T^5$
1e → *cis*-**2e** + *trans*-**2e** ($R^3 = CH_3$)	E + ZPVE[b]	−310.248671	−310.263576	−310.266318
	ZPVE[c]	409810.2	414846.9	414888.1
	$\langle S^2 \rangle$	0.7537	0.7540	0.7540
	$\Delta\Delta H_f$ [d]	≡ 0	−39.1	−46.3
	Conformer[e]	—[f]	$^3T_4$	$^3T_4$
1f → *cis*-**2f** + *trans*-**2f** [$R^3 = C(CH_3)_3$]	E + ZPVE[b]	−428.102026	−428.115379	−428.118958
	ZPVE[c]	632076.7	637519.0	638294.5
	$\langle S^2 \rangle$	0.7538	0.7541	0.7541
	$\Delta\Delta H_f$ [d]	≡ 0	−35.1	−44.5
	Conformer[e]	—[f]	$^3T_4$	$_4T^5$

[a] UB3LYP//6-31+G*//UB3LYP/6-31+G*. [b] E (not temperature corrected) + ZPVE in a.u.; 1 a.u. = 2625.50 kJ mol^{-1}. [c] ZPVE in J mol^{-1}. [d] $\Delta\Delta H_f$ in kJ mol^{-1} (ZPVE-corrected). [e] For cyclization products *cis*-**2** and *trans*-**2**. [f] For open chain conformers, see Fig. 1.

geometries of alkenoxyl radicals **1** and cyclized radicals *cis*/*trans*-**2** has been restricted for the sake of brevity to *tert*-butyl-substituted oxyl radicals **1b**, **1d**, **1f**, and tetrahydrofuryl-2-methyl radicals *cis*-**2b** and *trans*-**2b** (Fig. 1). The conformation of the 4-penten-1-oxyl radical chain and the positioning of substituents in methyl-substituted alkenoxyl radicals **1a**, **1c**, **1e** closely follows the information provided for the *tert*-butyl derivatives. Further structural details are evident from the information listed in Table 2.

Transition structures **7–10** were located on the corresponding potential energy surfaces as follows. One chair-like and one boat-like folding of the 4-penten-1-oxyl radical chain for the *cis-and* for the *trans*-5-*exo*-trig reaction served as input geometries. Substituents were positioned in either structure once in an equatorial and once in an axial position, thus providing a set of four transition structures. The argumentation for these, referring to the two most significantly populated intermediates per mode of ring closure is given in section 4 of the Discussion. A successive shortening of the distance O,C4 from 3.00 to 1.48 Å provided the highest energy structure along the reaction coordinate (AM1).[34] The maximum of this transit was taken as input for a subsequent transition structure search *via* gradient optimization procedures using the first and second derivatives at the DF level of theory. Verification of stationary points as authentic transition structures was achieved by vibrational analysis. The existence of one imaginary harmonic vibrational frequency that was associated with the trajectory of O,C4 bond formation classified intermediates **7–10** as authentic transition structures. DF-calculated heats of formation

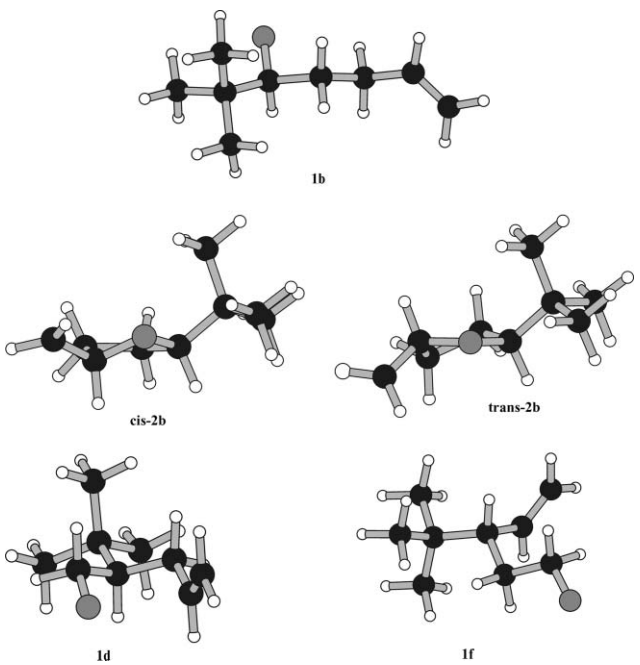

Fig. 1 Ball and stick presentation of computed equilibrium geometries of *tert*-butyl-substituted alkenoxyl radicals **1b** (top), **1d** and **1f** (bottom), and cyclization products *cis*/*trans*-**2b** (center). Oxygen atoms are depicted in grey, carbon atoms in black and hydrogen atoms in white.

Table 3 Calculated data, Maxwell–Boltzmann-weighted population P^a, and conformational details of transition structures **7–10**[a]

7–10	Data	**7**	**8**	**9**	**10**
a	E + ZPVE[b]	−310.244983	−310.243339	−310.246196	−310.241827
$R^1 = CH_3$	ZPVE[c]	412206.1	411965.7	412858.6	412071.1
	$\langle S^2 \rangle$	0.7789	0.7773	0.7784	0.7770
	$\Delta\Delta H_f$[d]	18.0	22.3	14.8	26.0
	G^{298}[e]	−310.276807	−310.275666	−310.278058	−310.274196
	ΔG^{298}[f]	3.3	6.3	≡ 0.0	10.1
	P^a [%][g]	19.3	5.84	73.62	1.23
	Conformer[i]	${}_2T^3$	${}_3T^4$	${}^2T_3$	${}^3T_4$
	Substituent[j]	*a/b*^{anticlinal}	*pe/pa*	*e/b*^{anticlinal}	*pa/pa*
b	E + ZPVE[b]	−428.098434	−428.100089	−428.102621	−428.096776
$R^1 = C(CH_3)_3$	ZPVE[c]	634812.0	634453.8	634788.5	635019.6
	$\langle S^2 \rangle$	0.7791	0.7756	0.7776	0.7715
	$\Delta\Delta H_f$[d]	27.2	22.9	16.2	31.6
	G^{298}[e]	−428.134987	428.137239	−428.139525	−428.133846
	ΔG^{298}[f]	11.9	6.0	≡ 0.0	14.9
	P^a [%][g]	0.71	8.01	90.99	0.22
	Conformer[i]	${}^3T_4$	${}_3T^4$	${}^2T_3$	${}_4T^5$
	Substituent[j]	*pa/pe*	*pe/pa*	*e/b*^{anticlinal}	*b/a*
c	E + ZPVE[b]	−310.243383	−310.236744	−310.241118	−310.240160
$R^2 = CH_3$	ZPVE[c]	412144.8	412286.4	412631.3	412031.6
	$\langle S^2 \rangle$	0.7787	0.7841	0.7784	0.7785
	$\Delta\Delta H_f$[d]	16.9	34.4	22.9	25.4
	G^{298}[e]	−310.275251	−310.268672	−310.272867	−310.272290
	ΔG^{298}[f]	≡ 0.0	17.3	6.3	7.8
	P^a [%][g]	88.93	0.08	7.12	3.89
	Conformer[i]	${}^2T_3$	${}_2T^3$	${}_2T^3$	${}_3T^4$
	Substituent[j]	*e/b*^{anticlinal}	*a/b*^{synclinal}	*a/b*^{anticlinal}	*e/pa*
d	E + ZPVE[b]	−428.096629	−428.087255	−428.092071	−428.093214
$R^2 = C(CH_3)_3$	ZPVE[c]	634914.9	634785.2	635724.4	634828.3
	$\langle S^2 \rangle$	0.7778	0.7837	0.7763	0.7763
	$\Delta\Delta H_f$[d]	7.8	32.4	19.7	16.7
	G^{298}[e]	−428.133749	−428.124636	−428.094401	−428.130411
	ΔG^{298}[f]	≡ 0.0	22.3	13.6	8.8
	P^a [%][g]	96.78	0.01	0.39	2.82
	Conformer[i]	${}^2T_3$	${}_1T^2$	${}_2T^3$	${}_3T^4$
	Substituent[j]	*e/b*^{anticlinal}	*pa/pe*	*a/b*^{anticlinal}	*e/pa*
e	E + ZPVE[b]	−310.238619	−310.237246	−310.241887	−310.237834
$R^2 = CH_3$	ZPVE[c]	413478.0	413120.4	412771.3	412412.7
	$\langle S^2 \rangle$	0.7791	0.7757	0.7784	0.7771
	$\Delta\Delta H_f$[d]	26.3	30.0	17.8	28.4
	G^{298}[e]	−310.270212	−310.269191	−310.273673	−310.269894
	ΔG^{298}[f]	9.1	11.8	≡ 0.0	9.9
	P^a [%][g]	2.34	0.83	95.09	1.74
	Conformer[i]	${}_2T^3$	${}_3T^4$	${}^2T_3$	${}^3T_4$
	Substituent[j]	*pa/b*^{anticlinal}	*e/pa*	*pe/b*^{anticlinal}	*a/pa*
f	E + ZPVE[b]	−428.084003	−428.090371	−428.095634	−428.089174
$R^3 = C(CH_3)_3$	ZPVE[c]	636501.8	636064.0	635416.4	635009.6
	$\langle S^2 \rangle$	0.7770	0.7727	0.7781	0.7827
	$\Delta\Delta H_f$[d]	47.3	30.6	16.8	33.7
	G^{298}[e]	−428.120153	−428.126971	−428.132355	−428.126427
	ΔG^{298}[f]	32.0	14.1	≡ 0.0	15.6
	P^a [%][g]	2.1×10^{-4}	0.33	99.48	0.19
	Conformer[i]	${}_2T^3$	${}_3T^4$	${}^2T_3$	${}_2T^3$
	Substituent[j]	*pa/b*^{anticlinal}	*e/pa*	*pe/b*^{anticlinal}	*pa/b*^{synclinal}

[a] UB3LYP//6-31+G*//UB3LYP/6-31+G*. [b] E (not temperature-corrected) + ZPVE in a.u.; 1 a.u. = 2625.50 kJ mol^{-1}. [c] ZPVE in J mol^{-1}. [d] $\Delta\Delta H_f$-values (ZPVE-corrected) in kJ mol^{-1}, referenced *versus* the associated alkenoxyl radical **1** (Table 2). [e] G^{298} in a.u. [f] ΔG^{298} in kJ mol^{-1}, referenced *versus* the lowest free-energy transition structure of every series of intermediates. [g] *P*. [h] [%] was calculated according to the following equation:

$$P^a = F^a \cdot 100 = 100 \cdot \left[\exp\{-\Delta G^a / RT\} \Big/ \sum_{i=1}^{4} \exp\{-\Delta G^i / RT\} \right].$$

[i] Classification of transition structures as distorted conformers of tetrahydrofuran (T = twist). [j] Arrangement of substituents in tetrahydrofuran-derived transition structures: $R^n/{=}CH_2$ (n = 1, 2, or 3; *a* = *axial*, *b* = *bisectional*, *e* = *equatorial*, *pa* = *pseudoaxial*, *pe* = *pseudoequatorial.* The notation *anticlinal–bisectional* (*b*^{anticlinal}) and *synclinal–bisectional* (*b*^{synclinal}) refers to the spatial arrangement of the $=CH_2$ entity. For definition of substituent positions refer to Fig. 4 and 5.

(E + ZPVE), zero-point vibrational energies (ZPVE), expectation values of spin operators ($\langle S^2 \rangle$), relative heats of formation ($\Delta\Delta H_f$), Gibbs free energies (G^{298}), ΔG^{298}-values, Maxwell–Boltzmann-weighted populations P^a (298.15 K), and a short summary of relevant conformational parameters of transition structures **7a–f**, **8a–f**, **9a–f**, and **10a–f** are summarized in Tables 3 and 4.

Table 4 Selected geometrical parameters of transition structures **7–10**[a]

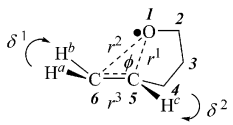

7–10

7–10	Parameter	7	8	9	10
a	r^1 [Å]	2.049	2.092	2.060	2.095
$R^1 = CH_3$	r^2 [Å]	2.665	2.659	2.649	2.655
	r^3 [Å]	1.377	1.372	1.374	1.371
	ϕ [°]	100.25	98.11	98.97	97.79
	δ^1 [°]	−174.20	−175.05	−174.22	−175.03
	δ^2 [°]	161.65	166.16	162.97	166.59
b	r^1 [Å]	2.073	2.097	2.067	2.134
$R^1 = C(CH_3)_3$	r^2 [Å]	2.692	2.672	2.655	2.698
	r^3 [Å]	1.373	1.370	1.374	1.365
	ϕ [°]	100.75	98.67	99.01	98.52
	δ^1 [°]	−175.23	−175.51	−174.32	−176.20
	δ^2 [°]	163.44	166.97	163.47	169.75
c	r^1 [Å]	2.051	2.061	2.053	2.066
$R^2 = CH_3$	r^2 [Å]	2.642	2.701	2.642	2.661
	r^3 [Å]	1.376	1.377	1.376	1.373
	ϕ [°]	98.98	101.75	98.91	98.46
	δ^1 [°]	−174.12	−175.14	−174.28	−174.92
	δ^2 [°]	162.43	161.52	162.44	165.50
d	r^1 [Å]	2.069	2.095	2.089	2.114
$R^2 = C(CH_3)_3$	r^2 [Å]	2.649	2.753	2.654	2.686
	r^3 [Å]	1.373	1.370	1.371	1.369
	ϕ [°]	98.62	103.21	98.04	98.66
	δ^1 [°]	−174.5	−175.06	−174.99	−175.55
	δ^2 [°]	163.48	161.75	164.52	167.32
e	r^1 [Å]	2.041	1.997	2.049	2.093
$R^3 = CH_3$	r^2 [Å]	2.636	2.627	2.636	2.654
	r^3 [Å]	1.378	1.390	1.375	1.372
	ϕ [°]	99.02	100.15	98.78	97.78
	δ^1 [°]	−173.57	−171.36	−174.05	−175.17
	δ^2 [°]	161.15	157.77	161.26	165.72
f	r^1 [Å]	2.044	2.076	2.051	2.072
$R^3 = C(CH_3)_3$	r^2 [Å]	2.559	2.573	2.614	2.658
	r^3 [Å]	1.377	1.372	1.375	1.374
	ϕ [°]	94.82	94.29	97.53	98.93
	δ^1 [°]	−172.86	−173.94	−174.11	−173.97
	δ^2 [°]	162.86	167.62	162.78	162.49

[a] r^1 = O1–C5, r^2 = O1–C6, r^3 = C5–C6, ϕ = O1–C5–C6, δ^1 = C5–C6–H^a–H^b, δ^2 = C6–C5–C4–H^c.

The illustration of transition structures outlined in Fig. 2 has, for the sake of brevity, been restricted to representative intermediates from the *cis*- and the *trans*-5-*exo*-trig cyclization of the 1-(*tert*-butyl)-4-pentenoxyl radical **1b**. A match plot showing intermediates from each favored mode of 5-*exo*-trig ring closure of radical **1a** (yellow) and 1-*tert*-butyl derivative **1b** (blue) is outlined in Fig. 3.

Discussion

1. Stereoselective tetrahydrofuran synthesis

(a) Alkenoxyl radical cyclizations. The customary *cis* selectivity in 5-*exo*-trig ring closures of 2-substituted 4-penten-1-oxyl radicals is retained in the intramolecular addition of 2-*tert*-butyl-substituted *O*-radical **1d**. Its diastereoselection (*cis* : *trans* = 90 : 10) exceeds the value measured for the 2-phenyl- (*cis* : *trans* = 88 : 12) and for the 2-methyl-derivative (*cis* : *trans* = 75 : 25) in the same temperature range.[3,30] A *tert*-butyl group at position 3 induces *trans*-selective tetrahydrofuryl-2-methyl radical formation, which qualitatively follows the trend observed for other 3-substituted 4-penten-1-oxyl radicals.[3,30] The degree of diastereoselection thereby increases along the series of 3-substituents CH_3 (*cis* : *trans* = 14 : 86) < C_6H_5 (*cis* : *trans* = 2 : 98) < $C(CH_3)_3$ (*cis* : *trans* < 2 : 98).

The concentration of the trapping reagent Bu_3SnH applied in the synthesis of *tert*-butyl-substituted tetrahydrofurans **3d** and **3f** correlates with the value established in previous kinetic experiments.[2,35] By comparing ratios of cyclized products **3** *versus* those of direct hydrogen atom trapping, *i.e.* *tert*-butyl-substituted bishomoallylic alcohols, it is therefore possible to estimate the magnitude of associated rate constants. Since relative yields of 2-(*tert*-butyl)-4-penten-1-ol and that of 3-(*tert*-butyl)-4-penten-1-ol did not exceed 2% (NMR analysis), it is reasonable to assume that the rate constants **1d** → *cis*/*trans*-**2d** and **1f** → *cis*/*trans*-**2f**

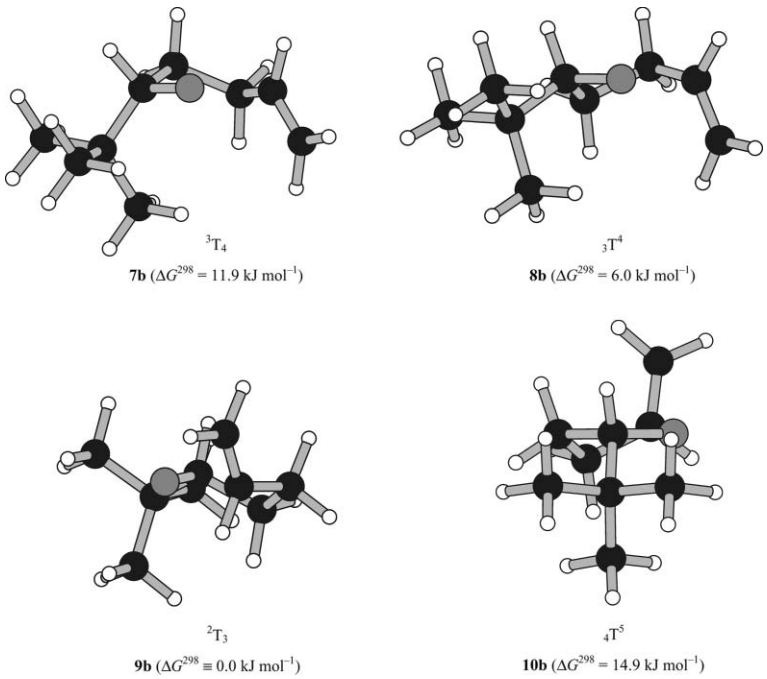

Fig. 2 Relevant transition structures (UB3LYP/6-31+G*) for the *cis*- (top) and the *trans*-5-*exo*-trig ring closure of the 1-(*tert*-butyl)-4-penten-1-oxyl radical **1b** (bottom). Oxygen atoms are depicted in grey, carbon atoms in black and hydrogen atoms in white.

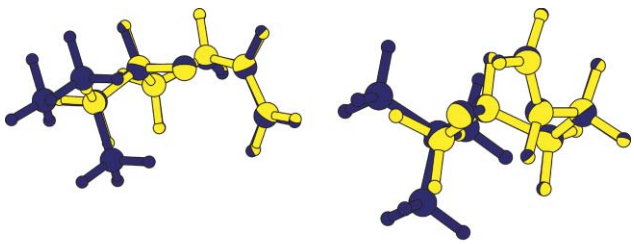

Fig. 3 Match plot of favored transition structures for the *cis*- (left) and the *trans*-5-*exo*-trig cyclization of 1-substituted 4-pentenoxyl radicals **1a** (yellow) and **1b** (blue).

are in the same order of magnitude ($k^{5\text{-}exo} \sim 10^8$ s^{-1} at ambient temperature) as those of their methyl-substituted derivatives, *i.e.* alkenoxyl radicals **1c** and **1e**.

(b) Stereochemical analysis. The *cis* configuration of the major cyclization product that is formed in the radical reaction between *N*-[(2-*tert*-butyl)pentenoxy]thiazolethione **6d** and Bu_3SnH, was determined on the basis of NOESY correlations. This information was supplemented by a stereochemical analysis on 4-(*tert*-butyl)-2-(iodomethyl)tetrahydrofuran (*cis* : *trans* = 91 : 9), which has been converted into 4-(*tert*-butyl)-2-methyltetrahydrofuran (**3d**) with a retention of relative configuration upon treatment with $LiAlH_4$/LiH (ESI†). The major stereoisomer of the iodomethyl compound showed a shift difference of 0.72 ppm for the two protons attached at C3. The minor stereoisomer showed a $\Delta\delta$ of 0.39 ppm. On the basis of a combined NMR–X-ray diffraction study on 4-substituted 2-(iodomethyl)tetrahydrofurans, the former value is indicative of a 2,4-*cis* configuration, whereas the latter points to a 2,4-*trans* arrangement.[6,36]

The *trans* arrangement of substituents in tetrahydrofuran *trans*-(**3f**), *i.e.* the product that is formed from *N*-[3-(*tert*-butyl)-pentenoxy]thiazolethione **6f** and Bu_3SnH, was determined as follows. Diastereomerically pure 3-(*tert*-butyl)-2-(iodomethyl)-tetrahydrofuran was prepared *via* iodocyclization of 3-*tert*-butyl-4-penten-1-ol in CH_3CN/satd. aq. $NaHCO_3$. The latter reaction has been investigated in great detail for the 3-phenyl derivative thus showing a marked 2,3-*trans* diastereoselectivity.[6] On the basis of results from a combined NMR–X-ray diffraction study,[6] the chemical shift of 13.5 ppm for the CH_2I carbon atom recorded for the sample of 3-(*tert*-butyl)-2-(iodomethyl)tetrahydrofuran is indicative of a 2,3-*trans* configuration. The corresponding ^{13}C resonance of the *cis*-isomer would have been expected at 6 ppm.[6] LiH/$LiAlH_4$-reduction of *trans*-3-(*tert*-butyl)-2-(iodomethyl)-tetrahydrofuran affords *trans*-**3f** (ESI†).

2 Calculated geometries of alkoxyl radicals 1 and cyclized radicals 2

(a) Alkenoxyl radicals 1. The atoms within the 4-pentenoxy chain of 1-substituted radicals (*R*)-**1a**, (*S*)-**1b** (Fig. 1), and the (2*S*)-methyl-4-pentenoxyl radical (*S*)-**1c** show a negative (−) *synclinal* (−*sc*) arrangement for O–C1–C2–C3, *antiperiplanar* (*ap*) for C1–C2–C3–C4, and *anticlinal* (*ac*) for C2–C3–C4–C5 (for atom count refer to Fig. 5). The −*sc*, +*sc*, *ac* arrangement of corresponding atoms in the favored conformation of 2-*tert*-butyl substituted radical (*R*)-**1d** gives rise to close contacts since the distances O···C4 = 2.624 Å and O···C5 = 3.036 Å fall below the sum of the associated van der Waals radii (1.52 Å for O and 1.70 Å for C, see below).[37] 3-Substituted alkenoxyl radicals (*S*)-**1e**, and (*S*)-**1f** (Fig. 1) are characterized by an *ap*, +*sc*, −*ac* orientation of atoms along the 4-pentenoxyl radical chain.

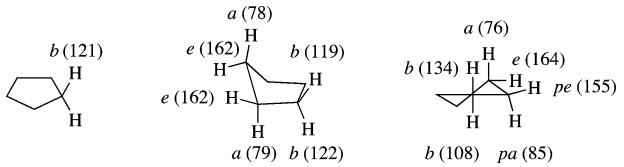

Fig. 4 Definition of H atom sites and calculated H–C–C–C dihedral angles [°] in distinguished conformers of cyclopentane (B3LYP/6-31+G*, ESI†): *equatorial* (*e*, 162–164°), *pseudoequatorial* (*pe*, 155°), *bisectional* (*b*, 134–108°), *pseudoaxial* (*pa*, 85°), and *axial* (*a*, 79–76). For cyclohexane: 177° for *e* and 66° for *a* (B3LYP/6-31+G*, ESI).[38,47]

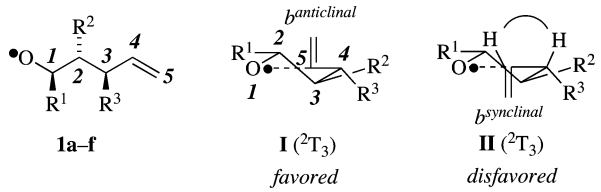

Fig. 5 Atom count in alkoxyl radical **1** (left) and tetrahydrofuran-derived transition structures, *e.g.* **I** and **II** (center and right). The curves in intermediate **II** symbolizes an approximately *synperiplanar* arrangement of substituents.

(b) Cyclization products. The heterocyclic core of substituted tetrahydrofuryl-2-methyl radicals **2** adopts twist (T) conformations.[38] The atoms that define a plane and those which are offset, however, differ, depending on the positioning and the steric size of substituents. The preference for the $_3T^4$ or $^3T_4$ conformation of tetrahydrofuran[39,40] is retained in most (*trans*-**2a**, *trans*-**2b**, *cis*-**2c**, *trans*-**2c**, *cis*-**2e**, *trans*-**2e**, *cis*-**2f**) but not all instances ($^1T_5$ for *cis*-**2a** and *cis*-**2b**, $^2T_3$ for *cis*-**2d**, $_1T^5$ for *trans*-**2d**, and $_4T^5$ for *trans*-**2f**). These arrangements may be rationalized on the basis of strain effects associated with the heterocyclic core *and* synclinal interactions caused by alkyl *and* CH_2 substituent positioning. The steric demand of substituents attached to tetrahydrofuran in radicals **2** follows the sequence $C(CH_3)_3 > CH_3 > CH_2$. The preference for placing an alkyl substituent in tetrahydrofuran, according to the data of the present study, decreases along the series of substituent arrangements $e > pe > b > pa > a$.[41–43] If related to H–C–C–C angles in distinguished conformers of cyclopentane[44–47] (B3LYP/6-31+G*, Fig. 4, ESI†), this sequence correlates with the magnitude of the dihedral angle that defines the offset of the substituent from a three atom segment of the heterocycle core. A larger dihedral angle, as a matter of fact, allows sterically demanding substituents to be directed further away from the cyclic framework thus reducing steric interactions between the two entities.

3 Reaction enthalpies

Results from DF calculations predict that 5-*exo*-trig cyclizations of methyl- and *tert*-butyl-substituted 4-penten-1-oxyl radicals **1a–f** are exothermic by −43 to −50 kJ mol^{-1}. Although it is tempting to interpret these numbers in terms of a notable barrier for the reverse reaction, absolute reaction enthalpies computed at the selected level of theory should be treated with care.[22] The calculated values are close to the range of −42 to −48 kJ mol^{-1} reported previously for 5-*exo*-trig cyclizations of 4-substituted 4-penten-1-oxyl radicals, but less exothermic than the number calculated for the methoxyl radical addition to the terminal position of propene (−61 kJ mol^{-1}) using the same computational method.[14]

The calculated relative heats of formation are in favor of 2,5-*trans* [$\Delta\Delta H_f = 0.9$ kJ mol^{-1} for **2a** and 0.5 kJ mol^{-1} for **2b**], 2,4-*cis* [$\Delta\Delta H_f = 2.9$ kJ mol^{-1} for **2c** and 2.3 kJ mol^{-1} for **2d**], and 2,3-*trans* cyclization products [$\Delta\Delta H_f = 7.2$ kJ mol^{-1} for **2e** and 9.4 kJ mol^{-1} for **2f**].

4 Transition structures, activation enthalpies, and computed selectivities

Stereoselectivities in 5-*exo*-trig cyclizations of methyl- and *tert*-butyl-substituted 4-penten-1-oxyl radicals were calculated by considering relative free energies of relevant transition structures **7–10** and Maxwell–Boltzmann statistics. This approach required simplifications to be made, which relate to temperature effects and the correlation between data from experiments to those from theory.

(i) Temperature effects in diastereoselective tetrahydrofuran synthesis *via* 4-penten-1-oxyl radical 5-*exo*-trig ring closures in the range of 15–30 °C are in most instances smaller than the necessary precision for experimentally determining such ratios.[2,3,30]

(ii) Correlation between theory and experiment: hydrogen atom delivery onto structurally simple primary, secondary, and tertiary alkyl radicals with Bu_3SnH proceeds with comparable rate constants.[48] Disubstituted tetrahydrofuran formation from either diastereomer of cyclized radicals **2a–f** and Bu_3SnH therefore is expected to occur with a similar efficiency and yield.

(a) Conformational and structural aspects of calculated transition structures. Two relevant transition structures for the *cis*- and two for the *trans*-5-*exo*-trig ring closure were located on potential energy surfaces of 4-penten-1-oxyl radicals **1a–f**. These structures are considered to represent the most significantly populated intermediates for the following reasons:

(i) If classified as distorted conformers of tetrahydrofuran, transition structures **7–10** adopt either low-energy conformers ($^2T_3$, $_2T^3$) or global minima ($_3T^4$, $^3T_4$). The fact that $^2T_3$-arranged intermediate **I** is consistently favored is explicable on the basis of conformational preferences and stereoelectronic effects.[49] An approach of reacting entities in a folded conformer, similar to the equilibrium structure of **1d** (Fig. 1) directly affords the underlying geometry of transition structure **I**, without undergoing further notable changes. The angle O1 ··· C5=C6 for **9a–b**, **7c–d**, **9e–f** measures 97.5–99.0°, which is in line with a Bürgi–Dunitz-type trajectory for the intramolecular *O*-radical addition.[50] The distance O1 ··· C5 in these intermediates (2.05–2.07 Å) points to tighter transition structures with a more acute angle of attack than those reported for 5-hexen-1-yl radical 5-*exo*-trig cyclizations.[13,12] On the basis of the present data and those which are disclosed in the ESI†, the preference for adopting $^2T_3$-arranged intermediates is considered to be only marginally dependent on the precise lengths of the newly formed bond, and hence the method applied for computing transition structures of 5-*exo*-trig cyclizations of alkenoxyl radicals **1** and structurally related derivatives thereof.

(ii) Substituents in favored transition structure **I** are located in *equatorial* (C2, C3), *pseudoequatorial* (C4), and *anticlinal–bisectional* (hereafter $b^{anticlinal}$, Fig. 5) positions. In intermediates with the next highest G^{298} value, the larger of the two substituents is found in one of the more favorable orientation, while the smaller

is located in one of the less favored ones (Fig. 6). The steric demand of substituents in the transition structures follows the alignment $C(CH_3)_3 > =CH_2 > CH_3$. The intermediate position of the $=CH_2$ substituent originates from stereoelectronic constraints associated with the C,O-bond formation. The preference for placing an alkyl substituent thereby decreases along the sites $e > pe > b > pa > a$.

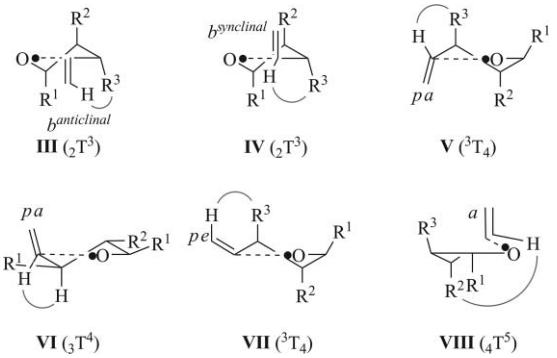

Fig. 6 Visualization of disfavored transition structures **III–VIII** in 4-penten-1-oxyl radical 5-*exo*-trig ring closures. Stereodescriptors refer to $=CH_2$ positioning. Curves symbolize an approximately *synperiplanar* arrangement of substituents.

(b) Activation enthalpies. The ring closure associated with the smallest activation enthalpy is correlated with major product formation, *i.e.* *trans*-**2a**, *trans*-**2b**, *cis*-**2c**, *cis*-**2d**, *trans*-**2e**, and *trans*-**2f**. These $\Delta H^{\ddagger}$-values fall into the range of 15–18 kJ mol^{-1} (for **1a–c**, **1e–f**). A smaller barrier for the *cis*-5-*exo*-trig reaction of 2-(*tert*-butyl)-substituted 4-pentenoxyl radical **1d** (8 kJ mol^{-1}) is considered to originate from its elevated ground state energy level caused by strain effects. Cyclizations associated with the next highest activation enthalpy afford products of opposed diastereoselection. Differences in enthalpic barriers between these two pathways increase along the series of substituents 1-CH_3 ($\Delta\Delta H^{\ddagger}$ = +3 kJ mol^{-1}), 2-CH_3 (+6 kJ mol^{-1}), 1-$C(CH_3)_3$ (+7 kJ mol^{-1}) < 3-CH_3 (+9 kJ mol^{-1}) ~2-$C(CH_3)_3$ (+9 kJ mol^{-1}) < 3-$C(CH_3)_3$ (+14 kJ mol^{-1}) and qualitatively reflect the degree of diastereoselection exerted by the given substituents at their positions.

(c) Stereoselectivities in 4-penten-1-oxyl 5-*exo*-trig ring closures. The 2,3-*trans*, 2,4-*cis*, and 2,5-*trans* diastereoselection exerted by a CH_3 or a $C(CH_3)_3$ group increases along positions 1 < 2 < 3 of the 4-penten-1-oxyl radical chain. This alignment correlates with the distance between the given substituents and the $=CH_2$ entity in 5-*exo*-trig transition structures. It differs, however, from the sequence 2 < 3 < 1 associated with steric effects of CH_3 and $C(CH_3)_3$ substituents in tetrahydropyran, as documented on the basis of experimental[51] and computational[52,53] (B3LYP/6-31+G*, ESI†) *A*-values analyses.

Theory slightly but systematically overestimates diastereoselection in 4-penten-1-oxyl radical 5-*exo*-trig reactions (298 K), if compared to experimentally determined *cis–trans* ratios of cyclic ethers **3a–f** (293–303 K, Table 5). One of the reasons for this deviation could be associated with the issue of conformer equilibration prior to C,O-bond formation as outlined above. If rate constants for conformational interchanges that are necessary in order to maintain the equilibrium of relevant transition structures come close to the rate constant of a 5-*exo*-trig ring closure, a depletion of lowest energy transition structures occurs. As a matter of fact, the statistical weight of cyclizations associated with the higher free-energy transition structures increases and becomes larger than the value calculated by Maxwell–Boltzmann statistics.

5 Diastereoselection in 4-penten-1-oxyl radical 5-*exo*-trig cyclizations

(a) The preferred path of 5-*exo*-trig ring closure. Theory predicts that the lowest free-energy transition structure in the 4-penten-1-oxyl radical 5-*exo*-trig ring closure adopts a distorted $^2T_3$ conformation of tetrahydrofuran. This intermediate is characterized by one elongated C,O-bond and an orientation of substituents which allows them to experience the fewest and least severe *synperiplanar* ($=CH_2$) and *synclinal* (CH_3 or $C(CH_3)_3$] interactions. Diastereoselection in cyclizations of the selected set of radicals thus originates from free-energy differences caused by strain effects within the distorted tetrahydrofuran nucleus and steric repulsions due to substituents attached to it.

(b) Scope and limitations. Multiple alkyl-substitution should be treated cumulatively, by positioning the majority of substituents into favored positions of a $^2T_3$-configured transition structure and

Table 5 Experimental and calculated stereoselectivities in cyclizations of 4-penten-1-oxyl radicals **1a–f**

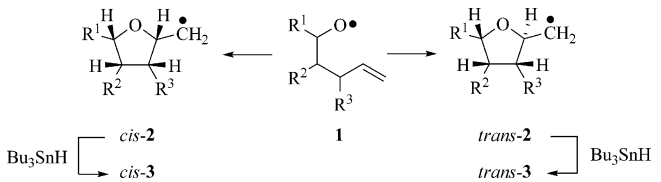

Entry	**1–3**	R^1	R^2	R^3	*cis*-**3** : *trans*-**3** (exp.)	*cis*-**2** : *trans*-**2**[a] (calcd.)
1	**a**	CH_3	H	H	36 : 64[b]	25 : 75
2	**b**	$C(CH_3)_3$	H	H	15 : 85[b]	9 : 91
3	**c**	H	CH_3	H	75 : 25[b]	89 : 11
4	**d**	H	$C(CH_3)_3$	H	90 : 10[c]	97 : 3
5	**e**	H	H	CH_3	14 : 86[b]	3 : 97
6	**f**	H	H	$C(CH_3)_3$	<2 : 98[c,d]	0.3 : 99.7

[a] $T = 25$ °C (298.15 K). [b] $T = 30$ °C. [c] $T = 20$ °C. [d] *cis*-**3f** was not detected (^{1}H NMR).

the minority into those which are disfavored. If the number of substituents in favorable positions minus those in disfavored ones is larger than 1, diastereoselection may increase, depending on the exact nature of the substituent. If the number is 1 or below, the stereoselectivity exerted by the largest substituent may be retained or lowered, depending on the accurate size and nature of the additional substituent(s).[4] An extension of this picture to a preferred positioning of polar substituents, for instance of *O*-alkyl, *O*-acyl, or other heteroatom groups, is considered to experience limitations since, *e.g.* *exo*-anomeric or related stereoelectronic effects, have not been considered in the present model. This issue is under current investigation.

(c) Stereochemical analysis of an unsettled instance. In view of the correlation between theory and experiment, attempts were made to re-interpret diastereoselection of the 1-phenyl-4-penten-1-oxyl radical (**1g**) and that of *p*-substituted 1-aryl-4-penten-1-oxyl radicals, which has hitherto been difficult to rationalize on the basis of cyclohexane-derived transition state models.[3a,30,35] Radical **1g** cyclizes in a kinetically controlled reaction to furnish a 52 : 48 mixture of *cis*-**3g** : *trans*-**3g**, if trapped with reactive H-atom donors (Scheme 6).[30] Favored transition structure **Ig** and its stereochemical alternative **IIIg** were constructed by considering the guidelines given in section 4 of the Discussion. An UB3LYP/6-31+G* computational analysis indicated that a coplanar arrangement between the phenyl and the oxyl radical substituent in **Ig**, similar to the recommended preferred conformation of the cumyloxyl radical,[54] is not attainable without imposing additional strain caused by close contacts between one of the *ortho*-hydrogens and the adjacent equatorially positioned H atom. In transition structure **IIIg**, however, a *synperiplanar* positioning of the phenyl and the oxyl radical substituent is feasible, which affords a parallel arrangement of the phenyl and the vinyl group. Since structure **IIIg** lacks significant *synclinal* interactions, neither of the likewise constructed transition structures should be significantly favored. This interpretation would suggest an approximate uniform distribution of *cis–trans* diastereoisomers to form from the 5-*exo*-trig reaction.

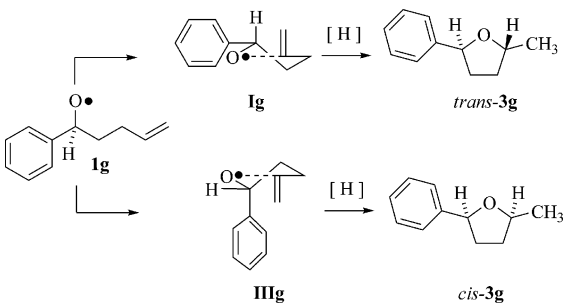

Scheme 6 Proposed energetically lowest transition structures **Ig** and **IIIg** in the 1-phenyl-4-penten-1-oxyl radical 5-*exo*-trig cyclization.

Concluding remarks

The favored mode of 5-*exo*-trig cyclization of methyl- and *tert*-butyl-substituted 4-penten-1-oxyl radicals proceeds, according to theory, *via* transition structures that show an offset of atoms C2 and C3 into opposite directions from the plane of O1 (radical center)/C5 (olefinic C)/C4 (allylic C). This conformation allows alkyl substituents and the $=CH_2$ entity to adopt positions that are associated with the fewest and least severe *synclinal* and *synperiplanar* interactions. Diastereoselection exerted by alkyl substituents thus originates from free-energy differences of relevant transition structures in 4-penten-1-oxyl radical 5-*exo*-trig ring closures, caused by strain effects within the distorted heterocyclic core and steric repulsion originating from substituents attached to it.

Finally, the transition structure notation applied in the present study deserves a comment. The systematic is based on the convention associated with the heterocycle, the intermediates structurally resemble the closest. This definitely is tetrahydrofuran and not tetrahydropyran. The selected approach will be illustrative for those who are familiar with the tetrahydrofuran and the furanose convention.[38] For those who feel more comfortable with the existing stereochemical model (Beckwith–Schiesser–Houk–Spellmeyer),[8,9] it should be added that most but not all selectivities in this study (see reactions of **1g**) could have been approximated using the latter mnemonic device. In recent years, however, it has become obvious from the literature that others have become aware of the dissimilarity between the geometry of computed transition structures in carbon radical cyclizations and the nomenclature they were using to describe these intermediates.[13] Although the authors consistently adhered to the common convention, it is essential to emphasize at this point that, at least for the 4-penten-1-oxyl radical 5-*exo*-trig cyclization, steric effects of alkyl substituents differ in degree and magnitude from what one would expect on the basis of an *A*-value analysis for tetrahydropyran. In view of these arguments we feel that the tetrahydrofuran-based transition state notation is able to more precisely refer to conformational aspects associated with the steric interplay between the distorted heterocyclic core and the substituents attached to it.

Experimental

Instrumentation and general remarks have been reported previously (see also the ESI†).[6]

1. Synthesis of thiohydroxamic acid *O*-esters—general procedure

A flame-dried round-bottomed flask was charged with anhydrous DMF (10 mL), *N*-(hydroxy)-4-(*p*-chlorophenyl)thiazole-2(3*H*)-thione tetraethylammonium salt (**4**) (1.07 g, 2.20 mmol) and treated at 20 °C in drops with a solution of alkenyl tosylate **5d** or **5f** (ESI†) (600 mg, 2.03 mmol) in anhydrous DMF (5 mL). The flask was wrapped in aluminium foil and stirring was continued for 6 d at 20 °C. The reaction mixture was poured into a mixture of *tert*-butyl methyl ether (MTB)–H_2O (30 mL each). The phases were separated. The aqueous layer was washed with MTB (3 × 20 mL). The organic phases were combined and washed with a satd. aq. solution of Na_2CO_3 (10 mL) and with brine (10 mL each) to afford a clear solution, which was dried ($MgSO_4$) and concentrated under reduced pressure. The remaining oil was purified by chromatography [SiO_2, petroleum ether–Et_2O = 1 : 1, (v/v)] to afford *N*-[(*tert*-butyl)pentenoxy)thiazolethione **6d** or **6f** as a colorless solid.

***N*-[2-(*tert*-Butyl)-4-penten-1-oxy]-4-(*p*-chlorophenyl)thiazole-2(3*H*)thione (5d).** Yield: 1.68 g (80%), mp 69 °C. ^{1}H NMR (250 MHz; $CDCl_3$): δ = 0.87 [s, 9 H, $C(CH_3)_3$], 1.35 (m_c, 1 H, 3-H), 1.75–1.91 (m, 1 H, 3-H), 2.10–2.22 (m, 1 H, 2-H), 3.89 (dd,

J 8.9, 4.9, 1 H, 1-H), 4.21 (dd, *J* 8.9, 4.9, 1 H, 1-H), 4.78 (ddd, *J* 15.6, 11.9, 1.5, 2 H, 4-H), 5.44 (m_c, 1 H, 5-H), 6.48 (s, 1 H, 5′-H), 7.47 (m_c, 4 H, Ar–H). ^{13}C NMR (63 MHz; $CDCl_3$): $\delta = 28.4$ (CH_3), 28.5 [$C(CH_3)_3$], 32.7 (C-2), 48.0 (C-3), 77.8 (C-1), 106.0 (C-5′), 116.1 (C-5), 127.1, 129.5 (Ph), 130.3 (Ph), 136.7, 138.0 (C-4′), 181.5 (C=S). IR (CCl_4): $\nu = 3108$, 2955, 2878, 1557, 1480, 1397, 1365, 1299, 1211, 1091, 1052, 1014, 959 cm^{-1}. MS (70 eV, EI): $m/z =$ 243 (9) [$C_9H_5ClNOS_2^+$], 168 (15) [$C_9H_5ClNS_2^+$], 84 (48), 57 (100), 41 (52). Calcd. for $C_{18}H_{22}ClNOS_2$ (367.95): C, 58.76; H, 6.03; N, 3.81; S, 17.43. Found: C, 58.78; H; 5.75; N, 3.91; S; 17.14%.

***N*-[3-(*tert*-Butyl)-4-penten-1-oxy]-4-(*p*-chlorophenyl)thiazole-2(3*H*)thione (6f).** Yield: 1.22 g (74%), mp 61 °C. ^{1}H NMR (250 MHz; $CDCl_3$): $\delta = 0.79$ [s, 9 H, $C(CH_3)_3$], 1.30 (dddd, *J* 13.7, 11.5, 9.5, 4.9, 1 H, 2-H), 1.60 (ddd, *J* 11.6, 9.5, 2.1, 1 H, 3-H), 1.85 (tdd, *J* 13.4, 7.9, 2.4, 1 H, 2-H), 3.94 (td, *J* 7.6, 7.3, 1 H, 1-H), 4.12 (dt, *J* 7.6, 4.9, 1 H, 1-H), 4.62 (dd, *J* 17.1, 2.1, 1 H, 5-H), 4.88 (dd, *J* 10.4, 2.1, 1 H, 5-H), 5.35 (ddd, *J* 17.1, 10.4, 9.8, 1 H, 4-H), 6.50 (s, 1 H, 5′-H), 7.50 (m_c, 4 H, Ar–H). ^{13}C NMR (63 MHz; $CDCl_3$): $\delta = 27.4$ [$C(CH_3)_3$)], 27.8 (CH_3), 31.2 (C-2), 51.3 (C-3), 76.3 (C-1), 105.9 (C-2′), 117.3 (C-4), 127.0, 129.5 (Ph), 130.1 (Ph), 136.0, 139.0, 171.95 (C=S). IR (KBr): $\nu = 2956$, 2870, 2357, 2334, 1792, 1645, 1554, 1481, 1453, 1308, 1204, 1040 cm^{-1}. MS (70 eV, EI): $m/z = 227$ (10) [$C_9H_5ClNS_2^+$], 168 (8) [$C_8H_5ClS^+$], 57 (100), 41 (24), 39 (17). Calcd. for $C_{18}H_{22}ClNOS_2$ (367.95): C, 58.76; H, 6.03; N, 3.81; S, 17.43. Found: C, 58.86; H, 5.94; N, 3.74; S, 17.96%.

2. Photolysis of *N*-[(*tert*-butyl)pentenoxy]-4-(*p*-chlorophenyl)-thiazole-2(3*H*)thiones 6 in the presence of Bu_3SnH (GC analysis)

A Schlenk flask was charged with a solution of *N*-(alkenoxy)-4-(*p*-chlorophenyl)thiazolethione **6d** or **6f** (25.5 mg, 0.066 mmol) in $C_6H_5CF_3$ (2 mL). Olefin-free tetradecane (8.3 mg, 0.042 mmol) was added (internal standard). The flask was sealed with a rubber septum and cooled to liquid-nitrogen temperature. The solution was deaerated by means of two freeze–pump–thaw cycles (Ar as flushing gas) and subsequently warmed in a water bath to 20 °C. Bu_3SnH (0.09 mL, 0.33 mmol) was added *via* a syringe. The reaction mixture was photolyzed for 25 min at 20 °C in a Rayonet® chamber photoreactor ($\lambda = 350$ nm) and hereafter analyzed by GC (for retention times and preparative scale synthesis of reference compounds refer to the ESI†).

3. Photolysis of *N*-[(*tert*-butyl)pentenoxy]-4-(*p*-chlorophenyl)-thiazole-2(3*H*)thiones 6 in the presence of Bu_3SnH (^{1}H NMR analysis)

A Schlenk flask was charged with a solution of *N*-(alkenoxy)-4-(*p*-chlorophenyl)thiazolethione **6d** or **6f** (25.5 mg, 0.066 mmol) in C_6D_6 (2 mL). A defined amount of anisole was added (internal standard). The flask was sealed with a rubber septum and cooled to liquid-nitrogen temperature. The reaction mixture was deaerated by means of two freeze–pump–thaw cycles (Ar as flushing gas) and was subsequently warmed in a water bath to 20 °C. Bu_3SnH (0.09 mL, 0.33 mmol) was added *via* a syringe. The colorless solution was photolyzed for 25 min in a Rayonet® chamber photoreactor ($\lambda = 350$ nm) and was subsequently analyzed by ^{1}H NMR (for spectral data of tetrahydrofurans **3d** and **3f** refer to the ESI†).

Acknowledgements

This work was generously supported by the Deutsche Forschungsgemeinschaft (Project Ha1705/3–2 and 3–3, and Graduiertenkolleg 690: Elektronendichte-Theorie und Experiment) and the Fonds der Chemischen Industrie.

References

1 For the discovery of the 4-penten-1-oxyl radical 5-*exo*-trig cyclization see: (*a*) J.-M. Surzur, M.-P. Bertrand and R. Nougier, *Tetrahedron Lett.*, 1969, 4197. For early work on the 4-penten-1-oxyl radical 5-*exo*-trig cyclization see: (*b*) R. D. Rieke and N. A. Moore, *J. Org. Chem.*, 1972, **37**, 413; (*c*) B. C. Gilbert, R. G. G. Holmes, H. A. H. Laue and R. O. C. Normann, *J. Chem. Soc., Perkin Trans. 2*, 1976, **2**, 1047; (*d*) A. L. J. Beckwith and B. P. Hay, *J. Am. Chem. Soc.*, 1988, **110**, 4415; (*e*) A. L. J. Beckwith, B. P. Hay and G. M. Williamson, *J. Chem. Soc., Chem. Commun.*, 1989, 1202.

2 For the discovery of stereoselective 4-penten-1-oxyl radical 5-*exo*-trig cyclizations see: J. Hartung and F. Gallou, *J. Org. Chem.*, 1995, **60**, 6706.

3 For reviews on the 4-penten-1-oxyl radical cyclization see: (*a*) J. Hartung, *Eur. J. Org. Chem.*, 2001, 619; (*b*) J. Hartung, in *Radicals in Organic Synthesis*, ed. P. Renaud and M. P. Sibi, Wiley-VCH, Weinheim, 2001, vol. 2, pp. 425–439.

4 J. Hartung and R. Kneuer, *Tetrahedron: Asymmetry*, 2003, **14**, 3019.

5 J. Hartung, T. Gottwald and K. Špehar, *Synthesis*, 2002, 1469.

6 J. Hartung, R. Kneuer, S. Laug, P. Schmidt, K. Špehar, I. Svoboda and H. Fuess, *Eur. J. Org. Chem.*, 2003, 4033.

7 (*a*) T. L. B. Boivin, *Tetrahedron*, 1987, **43**, 3309; (*b*) G. Cardillo and M. Orena, *Tetrahedron*, 1990, **46**, 3321; (*c*) J.-C. Harmange and B. Figadère, *Tetrahedron: Asymmetry*, 1993, **4**, 1711.

8 For a stereochemical model on the 5-hexen-1-yl radical cyclization see: (*a*) A. L. J. Beckwith and C. H. Schiesser, *Tetrahedron*, 1985, **41**, 3925; (*b*) A. L. J. Beckwith and J. Zimmermann, *J. Org. Chem.*, 1991, **56**, 5791.

9 (*a*) K. N. Houk, M. N. Paddon-Row, D. C. Spellmeyer, N. G. Rondan and S. Nagase, *J. Org. Chem.*, 1986, **51**, 2874; (*b*) D. C. Spellmeyer and K. N. Houk, *J. Org. Chem.*, 1987, **52**, 959.

10 D. P. Curran, N. A. Porter and B. Giese, *Stereochemistry of Radical Reactions*, Wiley-VCH, Weinheim, 1995.

11 For early work on the stereoselectivity of the 5-hexen-1-yl ring closure see: E. Canadell and J. Igual, *J. Chem. Soc., Perkin Trans. 2*, 1985, 1331.

12 J. Hartung, R. Stowasser, D. Vitt and G. Bringmann, *Angew. Chem., Int. Ed. Engl.*, 1996, **35**, 2820.

13 For recent computational studies on the 5-hexen-1-yl ring closure and related cyclizations see: (*a*) J. C. Tripp, C. H. Schiesser and D. P. Curran, *J. Am. Chem. Soc.*, 2005, **127**, 5518; (*b*) O. Corminboeuf, P. Renaud and C. H. Schiesser, *Chem.–Eur. J.*, 2003, **9**, 1578.

14 J. Hartung, R. Kneuer, C. Rummey and G. Bringmann, *J. Am. Chem. Soc.*, 2004, **126**, 12121.

15 B. J. Maxwell, B. J. Smith and J. Tsanaktsidis, *J. Chem. Soc., Perkin Trans. 2*, 2000, 425.

16 For recent work on related carbon radical cyclizations see: (*a*) I. V. Alabugin and M. Manoharan, *J. Am. Chem. Soc.*, 2005, **127**, 9534; (*b*) X. Guan, D. L. Philipps and D. Yang, *J. Org. Chem.*, 2006, **71**, 1984.

17 J. Hartung, M. Schwarz, I. Svoboda and H. Fuess, *Eur. J. Org. Chem.*, 1999, 1275.

18 (*a*) J. Hartung, in *Encyclopedia for Reagents in Organic Synthesis*, ed. L. Paquette, P. L. Fuchs, D. Crich and P. Wipf, John Wiley & Sons, New York, N. Y., 2004; (*b*) J. Hartung and M. Schwarz, *Org. Synth., Coll. Vol.*, ed. J. P. Freeman, John Wiley & Sons, New York, 2004, vol. 10, p. 437.

19 Y. Naruta, Y. Nishigaichi and K. Maruyama, *J. Org. Chem.*, 1991, **56**, 2011.

20 E. Montaudon, X. Lubeigt and B. Maillard, *J. Chem. Soc., Perkin Trans. 1*, 1991, 1531.

21 (*a*) D. E. Vogel and G. H. Büchi, *Org. Synth.*, 1993, **70**, 536; (*b*) W. S. Johnson, L. Werthemann, W. R. Barlett, T. J. Brockson, T.-T. Li, D. J. Faulkner and M. R. Peterson, *J. Am. Chem. Soc.*, 1970, **92**, 741.

22 (*a*) C. Barckholtz, T. A. Barckholtz and C. M. Hadad, *J. Phys. Chem.*, 2001, **105A**, 140; (*b*) A. Ricca and C. W. Bauschlicher, Jr., *Chem. Phys. Lett.*, 2000, **328**, 396; (*c*) J. R. Alvarez-Idaboy, N. Mora-Diez and

A. Vivier-Bunge, *J. Am. Chem. Soc.*, 2000, **122**, 3715; (*d*) M. W. Wong and L. Radom, *J. Phys. Chem.*, 1995, **99**, 8582; (*e*) R. Balderas-Gómez, M. L. Coote, D. J. Henry and L. Radom, *J. Phys. Chem.*, 2004, **108A**, 2874.
23 (*a*) B. S. Jursic, *J. Mol. Struct. (THEOCHEM)*, 1999, **492**, 285; (*b*) V. Van Speybroeck, Y. Borremans, D. Van Neck, M. Waroquier, S. Wauters, M. Saeys and G. B. Marin, *J. Phys. Chem.*, 2001, **105A**, 7713; (*c*) A. Milet and R. Arnaud, *J. Org. Chem.*, 2001, **66**, 6074.
24 A. D. Becke, *J. Chem. Phys.*, 1993, **98**, 5648–5652.
25 C. Lee, W. Yang and R. G. Parr, *Phys. Rev.*, 1998, **B37**, 785.
26 *Quantum chemical calculations were carried out on Intel LinuX Workstations using the Gaussian 98 (Revision A.7) software*, M. J. Frisch, G. W. Trucks, H. B. Schlegel, G. E. Scuseria, M. A. Robb, J. R. Cheeseman, V. G. Zakrzewski, J. A. Montgomery, Jr., R. E. Stratmann, J. C. Burant, S. Dapprich, J. M. Millam, A. D. Daniels, K. N. Kudin, M. C. Strain, O. Farkas, J. Tomasi, V. Barone, M. Cossi, R. Cammi, B. Mennucci, C. Pomelli, C. Adamo, S. Clifford, J. Ochterski, G. A. Petersson, P. Y. Ayala, Q. Cui, K. Morokuma, D. K. Malick, A. D. Rabuck, K. Raghavachari, J. B. Foresman, J. Cioslowski, J. V. Ortiz, A. G. Baboul, B. B. Stefanov, G. Liu, A. Liashenko, P. Piskorz, I. Komaromi, R. Gomperts, R. L. Martin, D. J. Fox, T. Keith, M. A. Al-Laham, C. Y. Peng, A. Nanayakkara, C. Gonzalez, M. Challacombe, P. M. W. Gill, B. Johnson, W. Chen, M. W. Wong, J. L. Andres, C. Gonzalez, M. Head-Gordon, E. S. Replogle and J. A. Pople, Gaussian, Inc., Pittsburgh, PA, 1998.
27 (*a*) R. Ditchfield, W. J. Hehre and J. A. Pople, *J. Chem. Phys.*, 1971, **54**, 724; (*b*) W. J. Hehre, R. Ditchfield and J. A. Pople, *J. Chem. Phys.*, 1972, **56**, 2257; (*c*) P. C. Hariharan and J. A. Pople, *Mol. Phys.*, 1974, **27**, 209.
28 H. Eyring, *J. Chem. Phys.*, 1935, **3**, 107.
29 D. Y. Curtin, *Rec. Chem. Prog.*, 1954, **15**, 111.
30 J. Hartung, M. Hiller and P. Schmidt, *Chem.–Eur. J.*, 1996, **2**, 1014.
31 The following rate constants for conformational changes about the central C,C bond in butane at 298.15 K have been estimated on the basis of the associated energy barriers: 1.4×10^{10} s^{-1} [$\Delta E = 15.1$ kJ mol^{-1}] for *antiperiplanar* → *synclinal* and for +*synclinal* → *synperiplanar* → −*synclinal*; 3.1×10^{9}–2.1×10^{8} s^{-1} [$\Delta E = 18.8$–25.5 kJ mol^{-1}] for *antiperiplanar* → *synperiplanar* → *synclinal*; E. L. Eliel, S. H. Wilen and L. N. Mander, *Stereochemistry of Organic Compounds*, J. Wiley, & Sons, New York, 1994, pp. 597–615.
32 HyperChem®, Version 4.5, Hypercube, Inc. MM+ supplements the Allinger's standard parameter for the MM2 force field (N. A. Allinger, *J. Am. Chem. Soc.*, 1977, **99**, 8127). All structures were taken from the molecule editor and optimized using the Fletcher–Reeves algorithm. Non-bonded electrostatic interactions were calculated as dipoles without cut-offs. Atom type O2 (ether oxygen) was applied for the *O*-radical center. For an assessment of the MM+ force field in conformational analysis see: A. Hocquet and M. Langgard, *J. Mol. Model.*, 1998, **4**, 94.
33 The energy criterion was set to 5 kcal mol^{-1}. Pre- and post optimization checks and duplication tests were carried out as suggested by Houk, Still, and coworkers: M. Saunders, K. N. Houk, Y.-D. Wu, C. W. Still, M. Lipton, G. Chang and W. C. Guida, *J. Am. Chem. Soc.*, 1990, **112**, 1419–1427.
34 M. J. S. Dewar, E. G. Zoebisch, E. F. Healy and J. J. P. Stewart, *J. Am. Chem. Soc.*, 1985, **107**, 3902.
35 J. Hartung, M. Hiller and P. Schmidt, *Liebigs Ann. Chem.*, 1996, 1425.
36 By mistake, the resonance of H-4 was omitted in the ^{1}H NMR spectral data of *cis*-2-(iodomethyl)-4-(2-naphthyl)tetrahydrofuran in ref. 6. The correct set of ^{1}H NMR data (250 MHz, $CDCl_3$) for this compound should read: $\delta_H = 1.94$ (ddd, *J* 9.2, 10.7, 12.5, 1 H, 3-H), 2.65 (ddd, *J* 5.8, 7.3, 12.8, 1 H, 3-H), 3.40 (dd, *J* 6.0, 10.1, 1 H, CH_2I), 3.43 (dd, *J* 5.2, 10.1, 1 H, CH_2I), 3.71 (dq, J_d 10.4, J_t 7.6 Hz, 1 H, 4-H), 4.04 (t, *J* 8.6, 1 H, 5-H), 4.22 (dq, J_d 9.5, J_q 6.1, 1 H, 2-H), 4.34 (t, *J* 8.5, 1 H, 5-H), 7.42 (dd, *J* 1.8, 8.6, 1 H, Ar-H), 7.47–7.54 (m, 2 H, Ar–H), 7.70 (m_c, 1 H, Ar-H), 7.79–7.87 (m, 3 H, Ar–H).
37 A. Bondi, *J. Chem. Phys.*, 1964, **68**, 441.
38 Nomenclature for twist and envelope conformers: superscripts are used for atoms which are displaced above the plane of three (T conformers) or four atoms (E conformer). Subscripts refer to atoms which are located underneath these planes. For a proper assignment of subscripts and superscripts of conformers, the atoms of the heterocyclic core, which define a plane, follow a clockwise arrangement with increasing atom count (*i.e.* O1–C2–C3): (*a*) C. Romers, C. Altona, H. R. Buys and E. Havinga, *Top. Stereochem.*, 1969, **4**, 39; (*b*) A. Zschunke, in *Molekülstruktur*, Spektrum Akademischer Verlag, Heidelberg, 1993, pp. 118–136.
39 R. Davidson and P. A. Warsop, *J. Chem. Soc., Faraday Trans.*, 1972, 1875.
40 (*a*) H. M. Seip, *Acta Chem. Scand.*, 1969, **23**, 2741; (*b*) S. J. Han and Y. K. Kang, *J. Mol. Struct. (THEOCHEM)*, 1996, **369**, 157.
41 B. Fuchs, *Top. Stereochem.*, 1978, **10**, 1.
42 C. K. Lee, *J. Korean Phys. Soc.*, 1999, **35**, 450–453.
43 J. Bogner, J. Delmau, J.-C. Duplan, Y. Infranet and J. Huet, *Bull. Soc. Chim. Fr.*, 1972, 3616.
44 (*a*) J. E. Kilpatrick, K. S. Pitzer and R. Spitzer, *J. Am. Chem. Soc.*, 1947, **69**, 2483; (*b*) K. S. Pitzer and W. E. Donath, *J. Am. Chem. Soc.*, 1959, **81**, 3213.
45 The expected *geometrical* changes upon substituting oxygen for CH_2 in cyclopentane are considered to be small.[40] The similarity between the carbocycle and the heterocycle, however, is restricted to structural parameter since it is known that relative conformational energies of substituted cyclopentanes and the corresponding tetrahydrofurans may differ considerably.[38,45].
46 B. Testa, *Grundlagen der Organischen Chemie*, VCH, Weinheim, 1983, p. 103.
47 By definition, *equatorial* and *axial* denote substituent positions in the undistorted chair conformation of cyclohexane. For reasons of simplicity, the classification of *equatorial* and *axial* sites in cyclopentane has been adapted on the basis of similar H–C–C–C dihedral angles to that of cyclohexane. In order to reproduce the values outlined for *e*, *pe*, *pa*, and *a* H atom sites, it is necessary to define the associated dihedral angle on the basis of C atoms from the puckered and *not* from the planar region. The scatter of data for the bisectional position comes by definition. A plane that bisects H–C–H angles and thus gives rise to bisectional H sites is found in all conformers of cyclopentane. The dihedral angles associated with the H atoms attached to the central C of the planar 3 atom fragment of a twist conformer, have to be defined by two atoms from a twist plane and a third, which is offset from this plane. The angle component of the offset is added to or subtracted from the expected value of *ca.* 120° thus leading to the observed values.
48 C. Chatgilialoglou, in *Radicals in Organic Synthesis*, ed. P. Renaud and M. P. Sibi, Wiley-VCH, Weinheim, 2001, vol. 1, pp. 28–49.
49 A. L. J. Beckwith, *Chem. Soc. Rev.*, 1993, **22**, 143.
50 A. J. Kirby, *Stereoelectronic Effects*, Oxford University Press, New York, 1996.
51 E. L. Eliel, K. D. Hargrave, K. M. Pietrusiewicz and M. Manoharan, *J. Am. Chem. Soc.*, 1982, **104**, 3635.
52 For a conformational analysis of 2-substituted tetrahydropyrans at the MP2 level of theory see: F. Freeman, M. L. Kasner and W. J. Hehre, *J. Mol. Struct. (THEOCHEM)*, 1999, **487**, 87.
53 For a conformational analysis of 3-substituted tetrahydropyrans at the MP2 level of theory see: F. Freeman, J. A. Kasner, M. L. Kasner and W. J. Hehre, *J. Mol. Struct. (THEOCHEM)*, 2000, **496**, 19.
54 D. V. Avila, K. U. Ingold, A. A. Dinardo, F. Zerbetto, M. Z. Zgierski and J. Lusztyk, *J. Am. Chem. Soc.*, 1995, **117**, 2711.

